α decay studies of very neutron-deficient francium and radium isotopes

J. Uusitalo,[1] M. Leino,[1] T. Enqvist,[1,*] K. Eskola,[2] T. Grahn,[1] P. T. Greenlees,[1] P. Jones,[1] R. Julin,[1] S. Juutinen,[1] A. Keenan,[1] H. Kettunen,[1] H. Koivisto,[1] P. Kuusiniemi,[1,†] A.-P. Leppänen,[1] P. Nieminen,[1,‡] J. Pakarinen,[1] P. Rahkila,[1] and C. Scholey[1]

[1]*Department of Physics, University of Jyväskylä, P.O. Box 35, FI-40014, Jyväskylä, Finland*

[2]*Department of Physics, University of Helsinki, FI-00014, Helsinki, Finland*

(Received 27 October 2004; published 11 February 2005)

Very neutron-deficient francium and radium isotopes have been produced in fusion evaporation reactions using ^{63}Cu and ^{65}Cu ions on ^{141}Pr targets and ^{36}Ar ions on ^{170}Yb targets. The gas-filled recoil separator RITU was employed to collect the fusion products and to separate them from the scattered beam. The activities were implanted into a position-sensitive silicon detector after passing through a gas-counter system. The isotopes were identified using spatial and time correlations between the implants and decays. Two new α decaying radium isotopes, ^{201}Ra and ^{202}Ra, were identified. The α decay energy and half-life of ^{203}Ra were measured with improved precision. The α decay properties measured for the francium isotopes ^{201}Fr, ^{202}Fr, ^{203}Fr, and ^{204}Fr were confirmed, in many cases with improved precision. For the first time, a $(\pi s_{1/2}^{-1})1/2^+$ proton intruder state was identified in francium isotopes, namely in ^{201}Fr and tentatively in ^{203}Fr. The measured decay properties for the neutron-deficient odd-mass Fr isotopes suggest an onset of substantial deformation at $N = 112$.

DOI: 10.1103/PhysRevC.71.024306 PACS number(s): 21.10.Dr, 23.60.+e, 27.80.+w

I. INTRODUCTION

Recently α decay has successfully been used to probe the nuclear structure above the $Z = 82$ shell closure [1,2]. The multiproton-multihole intruder states and the occurrence of shape coexistence have provided an interesting ground for detailed α decay fine structure studies in this region. In the translead region, due to the strong fission competition, in-beam γ-ray studies are often excluded. α decay studies after fast separation and performed far away from the production target allow higher beam intensities to be used. This together with the higher α-particle collection efficiency (when compared to the γ-ray collection efficiency) provides a viable means to obtain spectroscopic information even when the production cross sections are very low.

The α decaying $(\pi s_{1/2}^{-1})1/2^+$ proton intruder state has been shown to exist in many odd-mass bismuth and astatine nuclei [3–5]. A falling trend of excitation energy of the $(\pi s_{1/2}^{-1})1/2^+$ state as a function of decreasing neutron number has been observed. Actually the $(\pi s_{1/2}^{-1})1/2^+$ proton intruder state becomes the ground state in ^{195}At [4] and in ^{185}Bi [6,7]. This falling trend of the excitation energy as a function of decreasing neutron number is observed also for other single particle states such as the $(\pi i_{13/2})13/2^+$ state and the $(\pi f_{7/2})7/2^-$ state in odd-even nuclei and the $(\nu i_{13/2})13/2^+$ state in even-odd nuclei. The recent studies of the even-odd nuclei ^{191}Po [1] and ^{195}Rn [8] are good examples of such α decay studies. In the odd-odd nuclei the α decay studies could reveal quite complicated spectral structures for which the study of α decay chains of ^{206}Fr, ^{204}Fr, and ^{202}Fr is an excellent example [9]. For these odd-odd isotopes three different α decaying isomeric states $[\pi(h_{9/2})9/2^- \otimes \nu(i_{13/2})13/2^+]10^-$, $[\pi(h_{9/2})9/2^- \otimes \nu(f_{5/2})5/2^-]7^+$, and $[\pi(h_{9/2})9/2^- \otimes \nu(f_{5/2})5/2^-]2^+, 3^+$ have been reported [9].

In the present work, one of the goals has been to look for the possible proton $(\pi s_{1/2}^{-1})1/2^+$ intruder states in the odd-mass francium isotopes. In addition, the radium isotopes ^{204}Ra, ^{203}Ra, ^{202}Ra, and ^{201}Ra; the francium isotopes ^{204}Fr, ^{203}Fr, ^{202}Fr, and ^{201}Fr; and their descendant isotopes were studied using the α decay as a spectroscopic tool.

II. EXPERIMENTAL DETAILS

Three different heavy ion induced fusion evaporation reactions were used to synthesize neutron-deficient radium and francium isotopes studied in the present work. First, ^{65}Cu and ^{63}Cu beams were used on a ^{141}Pr target and, second, an ^{36}Ar beam was used on an ^{170}Yb target. The beams were delivered by the $K = 130$ MeV cyclotron of the Accelerator Laboratory at the Department of Physics of the University of Jyväskylä (JYFL). The fine adjustment of the bombarding energies was performed using a set of nickel and carbon foils in front of the target. Energy losses in the degrader foils, in the targets and in the helium gas filling of the separator were calculated using the TRIM code [10]. Typical copper beam intensities were 10–50 pnA and the total beam on target times were 52 and 125 h for ^{65}Cu and ^{63}Cu, respectively. Targets of rolled praseodymium of about 1-mg/cm^2 thickness were used in the copper bombardments. Typical argon beam intensities were 30–60 pnA and the total beam on target time was 52 h. With the argon beam rolled ytterbium targets of about 0.5-mg/cm^2 thickness enriched in ^{170}Yb (70%) were used.

The neutron-deficient francium and radium nuclides studied in this work were produced using projectile energies close to the Coulomb barrier. By minimizing the number of evaporation

*Present address: Department of Physics, University of Oulu, FI-90014, Oulu, Finland.

†Present address: Gesellschaft für Schwerionenforschung, D-64220 Darmstadt, Germany.

‡Present address: Australian National University, Canberra ACT0200, Australia.

 ©2005 The American Physical Society

steps the losses due to the strong fission competition are reduced.

Evaporation residues resulting from fusion reactions were separated from the beam using the JYFL gas-filled recoil separator RITU [11]. After passing through two multiwire proportional gas counters (MWPC) the residues were implanted into a position-sensitive silicon detector placed at the focal plane of RITU. The silicon detector (300 μm thick) is divided into 16 position-sensitive strips, and the total area of the detector is 35 $\times$ 80 mm^2. Because the vertical position resolution of each strip is better than 500 μm, the silicon detector can be treated as a pixel detector of more than 1000 pixels. Using spatial and time correlation, the implants were linked with their subsequent α decays and with α decays of their daughter nuclei. The recoil time-of-flight (TOF) measured using the gas counters combined with the recoil energy deposited in the silicon detector was used to separate the candidate fusion evaporation products from the scattered beam particles. In addition, the gas counters were used to separate the α particles from low-energy recoils. Behind the main silicon detector quadrant silicon detectors were used to veto energetic light particles punching through the first silicon detector. The pressure of the helium filling gas in RITU was typically 65 Pa (50 Pa when argon beam was used). The RITU gas volume was separated from the high vacuum of the beam line using a differential pumping system consisting of a Roots pump and collimators. The counting gas in the gas counter was isobutane of 300 Pa and the counter windows, made of 120-μg/cm^2 Mylar, were also used to keep the silicon detector chamber in high vacuum. The silicon detector was cooled down to 253 K using circulating alcohol. The events were gain matched and calibrated using well known α activities produced in the bombardments. For the energy calibration the α-particle energies taken from Refs. [12] and [13] are 5861.9(18) keV ^{200}Po, 6182.0(22) keV ^{198}Po, 6642.7(22) keV ^{199}At, 6917(3) keV ^{205}Fr, 7133(4) keV ^{203}Fr, 6772.1(25) keV ^{201}Rn, and 6902.4(25) keV ^{200}Rn. The full width at half maximum value with all 16 strips summed was measured to be 30 keV at the α-particle energy of 7000 keV.

III. RESULTS

Figure 1(a) presents the energy spectrum of all α particles observed in the silicon detector and vetoed with the gas counters and quadrant silicon detectors from ^{65}Cu+^{141}Pr reactions. Bombarding energies varied between $E_{\rm lab}$ = 283–293 MeV. The spectrum is dominated by activities formed in fusion channels involving charged particle evaporation. The strong α decay lines just above 5000 keV are due to the long-living ^{208}Po and ^{210}Po contaminants implanted into the detector in earlier experiments. These lines can be used to give some information about random correlation probabilities. In Fig. 1(b), only α decays correlated within 5 s with the implanted residues inside the proper recoil energy gates are shown. In this way the faster decaying activities are enhanced and the contaminant polonium lines are strongly reduced.

In Fig. 2, a two-dimensional energy plot is created by demanding that the correlated α decays are followed within

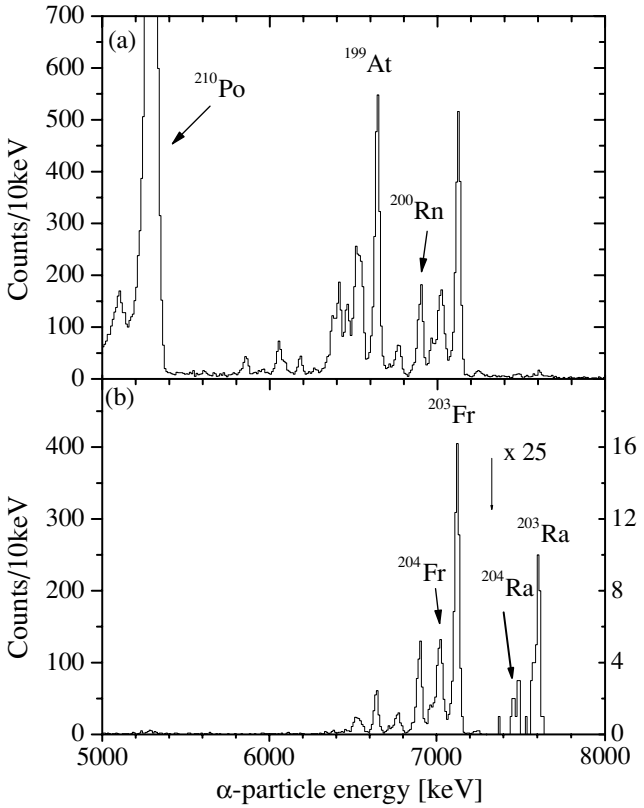

FIG. 1. Energy spectra of α particles measured in the silicon detector and vetoed with the gas counter using the ^{65}Cu+^{141}Pr reaction: (a) all decays and (b) decays following recoil implants within 5 s.

20 s by a second α decay. In this plot different isotopes can be recognized. The radon isotopes ^{201}Rn, ^{200}Rn, and ^{199}Rn produced in the αn, α2n, and α3n fusion-evaporation channels, respectively, can be identified. In the pn, p2n, and p3n fusion-evaporation channels the francium isotopes ^{204}Fr, ^{203}Fr, and ^{202}Fr were produced. Finally, the 2n and 3n fusion evaporation channels yielded the radium isotopes ^{204}Ra and ^{203}Ra. For the radium isotopes triple α decay chains, including the daughter activities ^{200}Rn and ^{199}Rn and granddaughter activities ^{196}Po and ^{195}Po, were identified and are illustrated in the two-dimensional plot Fig. 2.

For Figs. 3 and 4 the same conditions are valid as for Figs. 1 and 2. The only change is that ^{141}Pr targets were bombarded with a ^{63}Cu beam, again using bombarding energies close to the Coulomb barrier ($E_{\rm lab}$ = 278–288 MeV). Now the yield is more fragmented as expected, when trying to produce exotic nuclei further from the line of stability. As was illustrated above, in the two-dimensional energy plot different isotopes can be recognized. The radon isotopes ^{202}Rn, ^{201}Rn, ^{200}Rn, ^{199}Rn, and ^{198}Rn are now produced in the 2p, 2pn, 2p2n, αn, and α2n fusion-evaporation channels, respectively. The francium isotopes ^{202}Fr and ^{201}Fr are produced in the pn and p2n channels. The pure neutron-evaporation channels are very weak. However, two radium isotopes, the ^{202}Ra and ^{201}Ra produced in the 2n and 3n evaporation channels, respectively, can be identified.

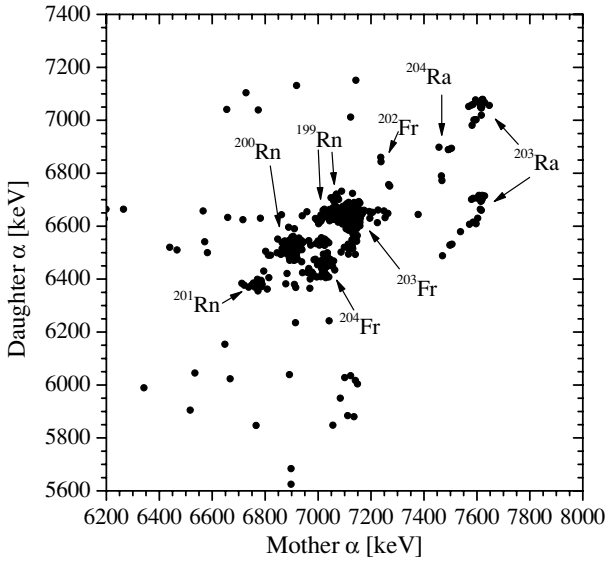

FIG. 2. Parent and daughter α-particle energies for all chains of the type ER-α_m-α_d observed in the ^{65}Cu+^{141}Pr irradiation. Maximum search times were 5 s for the ER-α_m pair and 20 s for the α_m-α_d pair.

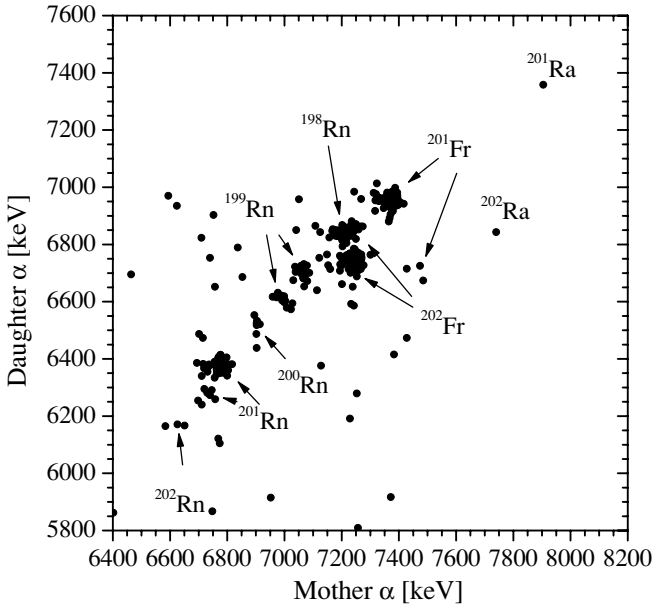

FIG. 4. Parent and daughter α-particle energies for all chains of the type ER-α_m-α_d observed in the ^{63}Cu+^{141}Pr irradiation. Maximum search times were 5 s for the ER-α_m pair and 20 s for the α_m-α_d pair.

The data are convincing, as can be seen in the two-dimensional plots with very low background. The single chains, originating from the ^{201}Ra, ^{202}Ra, and ^{201}Fr isotopes, will be discussed in more detail in the following. A triple α decay chain was observed, where the parent activity $E_\alpha =$ 7905 keV and $T_{\rm lt} = 2$ ms (lt denotes measured lifetime) was followed by a decay with $E_\alpha = 7358$ keV and $T_{\rm lt} = 48$ ms and by a third decay with $E_\alpha = 824$ keV (escape α particle) and $T_{\rm lt} = 96$ ms. We associate these measured values with the known activities of ^{197}Rn^m (from the $13/2^+$ isomeric state) with $E_\alpha = 7356(7)$ keV and $T_{1/2} = 19^{+8}_{-4}$ ms [14] and ^{193}Po^m (from the $13/2^+$ isomeric state) with $E_\alpha = 7004(5)$ keV and $T_{1/2} = 240(10)$ ms [13], and thus the activity with $E_\alpha =$ 7905 keV and $T_{\rm lt} = 2$ ms can be identified to originate from a new even-odd radium isotope ^{201}Ra.

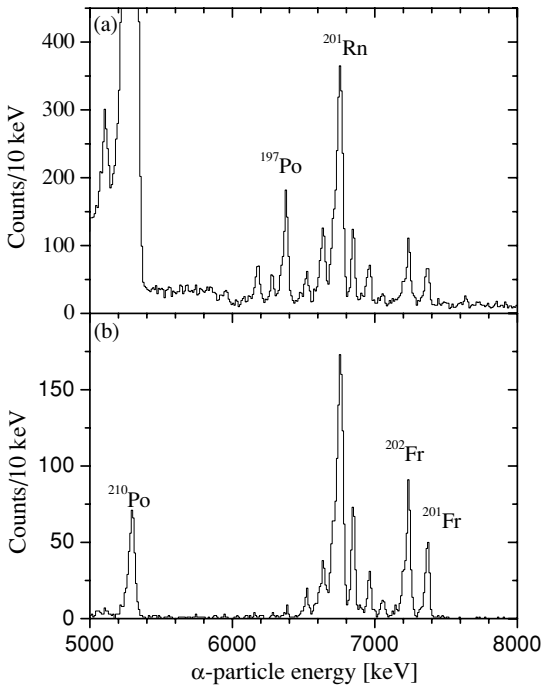

FIG. 3. Energy spectra of α particles measured in the silicon detector and vetoed with the gas counter using the ^{63}Cu+^{141}Pr reaction: (a) all decays and (b) decays following recoil implants within 5 s.

In a similar manner the parent activity with $E_\alpha = 7740$ keV and $T_{\rm lt} = 46$ ms was followed by a second decay with $E_\alpha =$ 2285 keV (escape α particle) and $T_{\rm lt} = 32$ ms and by a third decay with $E_\alpha = 6843$ keV and $T_{\rm lt} = 288$ ms. We associate these measured values with the known ground state to ground state (0^+ to 0^+) decays of ^{198}Rn with $E_\alpha = 7205(5)$ keV and $T_{1/2} = 64(2)$ ms [15] and ^{194}Po with $E_\alpha = 6842(6)$ keV and $T_{1/2} = 392(4)$ ms [13]. Thus the activity with $E_\alpha = 7740$ keV and $T_{\rm lt} = 46$ ms can be identified to originate from the (0^+) ground state of a new even-even isotope ^{202}Ra.

For the francium isotope ^{201}Fr two groups were identified. The bigger group represents the known $9/2^-$ ground state to $9/2^-$ ground-state α-particle decay [16]. The smaller group includes three events where the parent activity with $E_\alpha = 7462$ keV and $T_{\rm alt} = 33$ ms (alt denotes an average lifetime) was identified to be followed by a second decay with $E_\alpha = 6705$ keV and $T_{\rm alt} = 1.8$ s. One of these chains was identified to be followed by a third decay with $E_\alpha =$ 6481 keV and $T_{\rm lt} = 1.4$ s. The second decay in the chains can be recognized to belong to ^{197}At^m for which the decay properties with $E_\alpha = 6707(5)$ and $T_{1/2} = 2.0(2)$ s [17] have been reported to originate from an isomeric $1/2^+$ proton intruder state in ^{197}At. The third decay in one of the chains

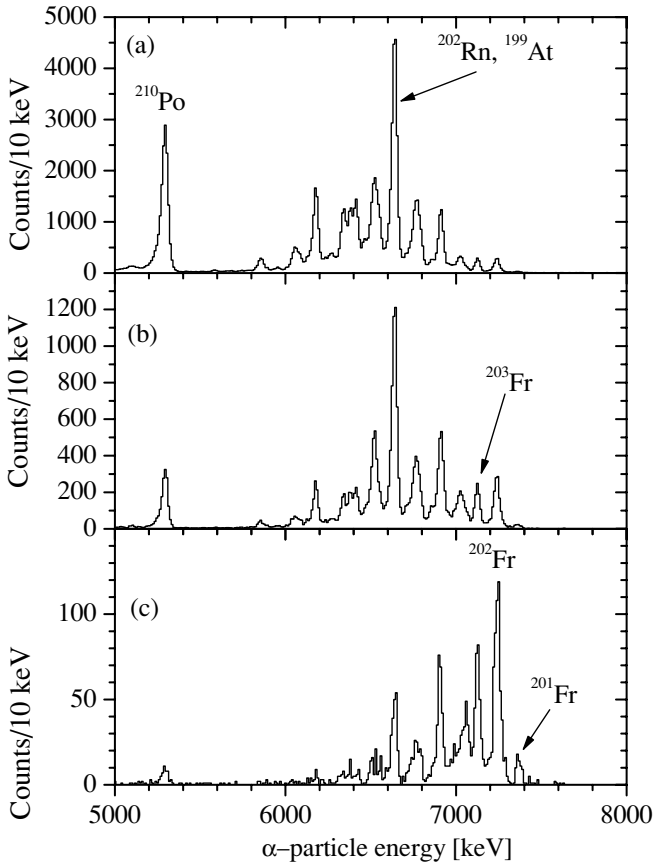

FIG. 5. Energy spectra of α particles measured in the silicon detector and vetoed with the gas counter using the ^{36}Ar+^{170}Yb reaction: (a) all decays; (b) decays following recoil implants within 2 s; (c) as (b) but followed by a second decay within 5 s.

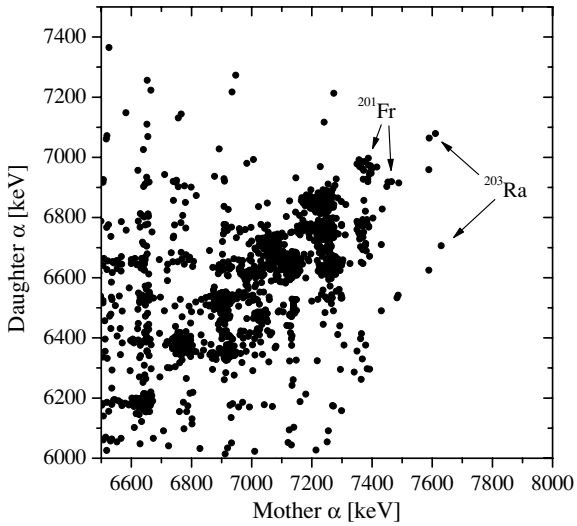

FIG. 6. Parent and daughter α-particle energies for all chains of the type ER-α_m-α_d observed in the ^{36}Ar + ^{170}Yb irradiation. Maximum search times were 2 s for the ER-α_m pair and 5 s for the α_m-α_d pair.

can be associated with ^{193}Bi^m for which the decay properties with $E_\alpha = 6475(5)$ keV and $T_{1/2} = 1.9(4)$ s [3] are reported for an isomeric $1/2^+$ proton intruder state. Therefore, the activity with $E_\alpha = 7462$ keV and $T_{\rm alt} = 33$ ms can be identified to originate from an isomeric $1/2^+$ state in ^{201}Fr. This is the first time when an α decay has been reported to originate from an $1/2^+$ proton intruder state in francium isotopes, as discussed later.

Figure 5(a) presents the energy spectrum of all α decays observed in the silicon detector and vetoed with the gas counters and quadrant silicon detectors using the ^{36}Ar +^{170}Yb reaction with all bombarding energies combined ($E_{\rm lab} =$ 180–185 MeV). As can be seen from the spectrum, the yield is more fragmented when compared to the Cu+Pr experiments. There are two reasons for that. First, even though bombarding energies close to the Coulomb-barrier energies were used the compound nuclei have more excitation energy due to the unfavorable mass differences. This leads to more particles being evaporated during the cooling process. Second, the ytterbium target was enriched to only 70% in mass 170, therefore including 30% of heavier ytterbium isotopes. This leads to extra yield of fusion residues due to smaller fission competition. In Fig. 5(b) only α decays correlated within 2 s with the implanted residues inside the proper recoil energy gates are shown. Figure 5(c) shows α decays with the additional requirement that the decays are followed within 5 s by α particles with energies between 5000 and 10000 keV. The effect of additional yield of fusion residues can be seen in spectrum (b). When the ^{210}Po α decay line is considered it can be seen that about 12% of the decays find a recoil with conditions used. These correlations are random. An additional requirement of a second decay drops this accidental rate down to a level well below 1%. This accidental rate goes rapidly down when faster decays are considered. In the correlation analysis only the first α decay after a recoil event is accepted.

Finally in Fig. 6 a two-dimensional energy plot is shown from where different isotopes can be recognized. This reaction yielded additional events for the isotopes ^{201}Fr and ^{203}Ra. For example, one triple α decay chain was found where the parent activity with $E_\alpha = 7431$ keV and $T_{\rm lt} = 10$ ms was followed by a second decay with $E_\alpha = 6710$ keV and $T_{\rm lt} = 689$ ms and by a third decay with $E_\alpha = 6490$ keV and $T_{\rm lt} = 3.7$ s. When these decay values are compared to the known decay properties measured for ^{197}At^m and ^{193}Bi^m, respectively, the decay with $E_\alpha = 7431$ keV and $T_{\rm lt} = 10$ ms can be identified to originate from the isomeric $1/2^+$ proton intruder state in ^{201}Fr.

When the efficiency of the RITU separator is assumed to be 30%, the radium isotopes were determined to be produced with the following cross sections: ^{204}Ra 0.7 nb, ^{203}Ra 4 nb, ^{202}Ra 25 pb, and ^{201}Ra 25 pb. The francium isotopes were produced with the following cross sections: ^{204}Fr 40 nb, ^{203}Fr 120 nb, ^{202}Fr 4 nb, and ^{201}Fr 3 nb. These cross-section values do not necessarily represent the maximum values because we did not run excitation functions.

IV. DISCUSSION

In the present work α decay hindrance factors HF and reduced widths δ^2, determined according to Rasmussen [18],

TABLE I. The α decay properties of the radium isotopes and their corresponding daughter and granddaughter isotopes observed in the present work. The literature values are taken from Refs. [13–15,22]. The α decay reduced widths δ^2 and half-lives normalized to ^{212}Po, calculated according to Ref. [18], are also given. Escaped α's are denoted by (esc).

Nuclide	E_α (keV)		$T_{1/2}$ (ms)			δ^2 (keV)	I^π
	Meas.	Lit.	Meas.	Lit.	Calc.		
^{201}Ra^m	7905(20)	—	$1.6^{+7.7}_{-0.7}$	—	3.1	141	$13/2^+$
^{197}Rn^m	7358(14)	7356(7)	30^{+150}_{-15}	19^{+8}_{-4}	32	121	$13/2^+$
^{193}Po^m	824 (esc)	7004(5)	70^{+330}_{-30}	240(10)	89	25	$13/2^+$
^{202}Ra	7740(20)	7860(60)	16^{+30}_{-7}	$0.7^{+3.3}_{-0.3}$	9.6	44	0^+
^{198}Rn	2285 (esc)	7205(5)	22^{+110}_{-10}	64(2)	106	120	0^+
^{194}Po	6843(14)	6842(6)	200^{+960}_{-90}	392(4)	313	58	0^+
^{203}Ra^m	7612(8)	7615(20)	24^{+6}_{-4}	33^{+22}_{-10}	24	71	$13/2^+$
^{199}Rn^m	7060(6)	7059(10)	260^{+80}_{-50}	325(25)	303	68	$13/2^+$
^{195}Po^m	6700(6)	6699(5)	$2.8^{+1.0}_{-0.6}$ s	1.92(2) s	0.99 s	34	$13/2^+$
^{203}Ra^g	7589(8)	7577(20)	31^{+17}_{-9}	$1.0^{+5.0}_{-0.5}$	28	66	$3/2^-$
^{199}Rn^g	6989(6)	6995(10)	$1.1^{+0.9}_{-0.4}$ s	0.620(25) s	0.520 s	60	$3/2^-$
^{195}Po^g	6617(6)	6606(5)	$3.9^{+3.2}_{-1.2}$ s	4.64(9) s	2.1 s	26	$3/2^-$
^{204}Ra	7486(8)	7484(10)	54^{+19}_{-11}	59^{+12}_{-9}	59	73	0^+
^{200}Rn	6903(6)	6902(3)	$1.1^{+0.6}_{-0.3}$ s	1.06(2) s	1.08 s	72	0^+
^{196}Po	6533(6)	6521(5)	$5.1^{+3.1}_{-1.4}$ s	5.8(2) s	4.7 s	55	0^+

are used to obtain structure information of the decaying states. The α decay properties of the radium isotopes and their corresponding daughter and granddaughter isotopes observed in the present work are summarized in Table I. Only data where the first decay has originated from a radium isotope are shown. The reduced width values shown in Table I are calculated taking into account the α decay branch values given in Ref. [19]. If the α decay branch is not known a 100% α decay branch value is used, which is a reasonably good approximation for most of the cases also when considering the predicted β decay half-life values given in Ref. [20]. The decay properties measured for the even-even nucleus ^{204}Ra and for the corresponding descendants ^{200}Rn and ^{196}Po are well compatible with the decay properties reported in the literature. All the decays in the chain represent unhindered 0^+ ground state to 0^+ ground-state transitions.

For ^{203}Ra two α decaying states were observed. When the hindrance factor is defined as the ratio of the reduced width of the ground-state-to-ground-state transition in the closest even-even neighbor to the reduced width of the transition in question, hindrance factors of 1.12 and 1.03 can be obtained. In odd-mass nuclei a hindrance factor less than 4 implies an unhindered α decay among states of equal spin, parity, and configuration [21]. Thus the 7589 keV α decay originates from the $(\nu p_{3/2})3/2^-$ ground state and the 7612 keV α decay originates from the $(\nu i_{13/2})13/2^+$ isomeric state of ^{203}Ra. Notice that for the ground-state decay only one event was known before with a decay time of about 1 ms [22] as illustrated in Table I.

The α decay properties measured for the isotope ^{202}Ra are not quite compatible with the decay values reported in Ref. [22]. The decay values given in Ref. [22] are based on one measured triple decay chain where both the daugher α particle and the granddaughter α particle escaped the detector. In addition, as it is pointed out in Ref. [22], the detector performance was reduced during the experiment, giving a quite poor energy resolution. Unfortunately again, only one chain was observed in the present work. This time the granddaughter decay was measured with full α-particle energy. With the improved detector performance the measured decay energy from the present work for the even-mass isotope ^{202}Ra can be considered to be more accurate than the previous value. Conversely, if we combine the decay time measured in the present work (46 ms) with that given in Ref. [22] (0.7 ms) a decay half-life of $T_{1/2} = 16$ ms can be obtained. If the decay half-life is $T_{1/2} = 16$ ms the probability to find a decay with a decay time shorter than 1 ms is 4% and the probability to find a decay with a decay time longer than 46 ms is 14%, both percentage values being high enough to be significant. Therefore in Table I the decay properties of ^{202}Ra are given so that the decay energy is taken from the present work and the decay half-life is combined using the decay times obtained in this work and that given in Ref. [22].

One α decay chain was obtained also for ^{201}Ra. The measured α decay chain is convincing and when the measured α decay half-life is compared to the calculated α decay half-life the decay can be considered unhindered. When this is added to the fact that this decay was followed by an α decay reported to originate from a $(\nu i_{13/2})13/2^+$ isomeric state in ^{197}Rn, the decay with $E_\alpha = 7905(20)$ keV can be assigned to originate from the corresponding $(\nu i_{13/2})13/2^+$ isomeric state in ^{201}Ra.

TABLE II. The α decay properties of the francium isotopes and their corresponding daughter and granddaughter isotopes observed in the present work. The literature values are taken from Ref. [3,9,12,17,26]. The α decay reduced widths δ^2 and half-lives normalized to ^{212}Po, calculated according to Ref. [18], are also given.

Nuclide	E_α (keV)		$T_{1/2}$ (s)			δ^2 (keV)	I $^{\pi}$
	Meas.	Lit.	Meas.	Lit.	Calc.		
^{204}Fr^m	7017(6)	7013(5)	0.8(2)	$\simeq$1	0.94	65 (50)	10^-
^{200}At^m	6534(6)	6538(3)	$7.3^{+2.6}_{-1.5}$	3.5(2)	9.9	21 (30)	10^-
^{204}Fr^m	6976(6)	6969(5)	$1.6^{+0.5}_{-0.3}$	2.6(3)	1.4	35 (50)	7^+
^{200}At^m	6413(6)	6411(2)	—	47(1)	31	20 (30)	7^+
^{204}Fr^g	7033(6)	7031(5)	1.9(5)	1.7(3)	0.84	34 (50)	3^+
^{200}At^g	6467(6)	6464(2)	—	43(1)	19	18 (30)	3^+
^{203}Fr^g	7130(6)	7133(4)	0.53(2)	0.560(15)	0.380	47 (50)	$9/2^-$
^{199}At^g	6643(6)	6643(3)	7.8(4)	6.92(15)	3.9	36 (30)	$9/2^-$
^{202}Fr^m	7235(8)	7237(8)	0.29(5)	0.34(4)	0.17	36 (71)	10^-
^{198}At^m	6850(6)	6856(4)	1.04(15)	1.0(2)	0.6	46 (39)	10^-
^{202}Fr^g	7241(8)	7237(8)	0.30(5)	0.34(4)	0.17	36 (71)	3^+
^{198}At^g	6748(6)	6755(4)	3.8(4)	4.2(3)	1.5	26 (39)	3^+
^{201}Fr^m	7454(8)	—	19^{+19}_{-6} ms	—	33 ms	126 (71)	$1/2^+$
^{197}At^m	6706(9)	6707(5)	$1.1^{+1.1}_{-0.4}$	2.0(2)	2.4	86 (39)	$1/2^+$
^{193}Bi^m	6481(14)	6475(5)	$1.4^{+3.8}_{-0.6}$	1.9(4)	2.8	98 (10)	$1/2^+$
^{201}Fr^g	7369(8)	7361(7)	53(4) ms	69^{+16}_{-11} ms	63 ms	86 (71)	$9/2^-$
^{197}At^g	6959(6)	6960(5)	0.34(2)	0.388(6)	0.29	57 (39)	$9/2^-$

The α decay properties of the francium isotopes studied and their corresponding daughter and granddaughter isotopes observed in the present work are summarized in Table II. Only data where the first α decay has originated from a francium isotope are shown. For the odd-odd isotope ^{204}Fr three α decaying isomeric states were observed. The measured α decay properties are well compatible with the values reported in Ref. [9]. As the present work is based on correlation chains, more detailed information can be extracted. For example, in this work for the $[\pi(h_{9/2})9/2^- \otimes \nu(i_{13/2})13/2^+]10^-$ isomeric state a more accurate α decay half-life was obtained.

For the odd-odd isotope ^{202}Fr and for the corresponding descendant only two α decaying isomeric states, $[\pi(h_{9/2})9/2^- \otimes \nu(i_{13/2})13/2^+]10^-$ and $[\pi(h_{9/2})9/2^- \otimes \nu(f_{5/2})5/2^-]3^+$, have been reported [9]. This was confirmed in the present work. As in Table I the reduced widths, shown in Table II, are calculated using the α decay branch values given in Ref. [19]. If not known an α decay branch value of 100% is used. For comparison the reduced width values calculated for the closest even-even neighbor are shown in brackets. For the closest even-even neighbor the smaller element number is used, because normally for those nuclei the α decay properties are known more precisely. Most of the calculated reduced width values lie between 20 and 90 keV. If these are compared to the reduced width values calculated for the closest even-even neighbors hindrance factor values of 0.8–2.0 can be obtained. This implies again unhindered α decays among states of equal spin, parity, and configuration. For example, for the decay of ^{200}At^m with $E_\alpha = 6534(6)$ keV a reduced width value of 21 keV is calculated taking into account the given 10.5% α decay branch [9]. In this case most of the decay proceeds via a slow electromagnetic transition (84%) [9,23]. Without knowing a this a reduced width value of 198 keV would result implying an unexpectedly fast α decay. In the present work from the crossing α decay chains an about 80% branch for the $E3$ transition can be obtained to occur between the $[\pi(h_{9/2})9/2^- \otimes \nu(i_{13/2})13/2^+]10^-$ and $[\pi(h_{9/2})9/2^- \otimes \nu(f_{5/2})5/2^-]7^+$ isomeric states in ^{200}At. This is in good agreement with the value 84% given in [9,23]. In the present estimate the β decay half-life value given in [20] has been taken into account.

The measured decay time for the $[\pi(h_{9/2})9/2^- \otimes \nu(i_{13/2})13/2^+]10^-$ isomeric state in ^{202}Fr indicates a much smaller $E3$ internal transition branch. Even though it could be impossible to measure this kind of slow highly converted $E3$ transition with such a low yield, it could speed up the decay of the level and show up as an unexpectedly fast α decay. This effect is not seen (as clearly) in the α decay of ^{202}Fr and its descendants. The decay of ^{198}At^m with $E_\alpha = 6850(6)$ keV is slightly faster than the other decays of ^{202}Fr and ^{198}At and this could be a sign of an $E3$ transition branch from this state. This, in addition to the nonexistence of the third α decaying isomeric state, is a fingerprint that the $[\pi(h_{9/2})9/2^- \otimes \nu(f_{5/2})5/2^-]7^+$ isomeric state does not show up in ^{202}Fr.

For the odd-even isotope ^{201}Fr two α decaying isomeric states were obtained. The earlier results where the α decay was taken to originate from the $(\pi h_{9/2})9/2^-$ state was confirmed in the present work. In addition a second α decay, identified

TABLE III. Observed α decay correlation chains that could not be linked to any known isotopes, except the first one which originates from the francium isotope ^{203}Fr.

E_α (keV)	$T_{1/2}$ (s)	E_α (keV)	$T_{1/2}$ (s)	Number of chains
7130(6)	0.53(2)	6643(6)	7.8(4)	688
7227(8)	$0.06^{+0.03}_{-0.02}$	6643(6)	$4.3^{+2.4}_{-1.1}$	8
7118(6)	$1.04^{+0.35}_{-0.21}$	6517(6)	$9.4^{+3.1}_{-1.9}$	16
7128(6)	$0.51^{+0.51}_{-0.17}$	6021(6)	$4.3^{+4.3}_{-1.4}$	4

to originate from an isomeric intruder $(\pi s_{1/2}^{-1})1/2^+$ state, was observed in the present work. This is the first time when an isomeric $(\pi s_{1/2}^{-1})1/2^+$ proton intruder state, known to exist in many neutron-deficient bismuth and astatine isotopes, is found in francium isotopes. The slightly high reduced width values obtained for the isotopes ^{193}Bi and ^{201}Fr could be a sign for a competing $E3$ transition from these states. This could happen if the $(\pi f_{7/2})7/2^-$ state, identified in the heavier isotopes, falls below the $(\pi s_{1/2}^{-1})1/2^+$ state. The above situation was recently demonstrated to occur in ^{191}Bi, where the $7/2^-$ state lies 93 keV below the $1/2^+$ isomeric intruder state shortening the decay time of the state [4]. In ^{197}At the $(\pi f_{7/2})7/2^-$ state has to lie above the $(\pi s_{1/2}^{-1})1/2^+$ intruder state because a half-life of 2.0 s has been measured for this α decaying state. (In Ref. [4] the $7/2^-$ state is presented as a $7/2^-[514]$ Nilsson state but in this work the $7/2^-$ state is presented as a $(\pi f_{7/2})7/2^-$ shell model state.)

In Table III all the found correlation chains that could not immediately be linked to any known isotope are collected. In addition, for comparison the $(\pi h_{9/2})9/2^-$ ground state to the $(\pi h_{9/2})9/2^-$ ground state α decay, known in ^{203}Fr, is shown. The recently found isomeric $M2$ transition ($13/2^+$ to $9/2^-$) in ^{199}At [24] gives additional support that the ground-state spin and parity really is $9/2^-$ in ^{199}At. The unhindered α decay to this state gives some further proof on that the ground-state spin and parity remain $9/2^-$ in ^{203}Fr. The same statement is valid also for the isotope ^{201}Fr because a similar isomeric $M2$ transition has recently been reported to exist in the ^{197}At daughter nucleus [17].

There is some evidence that the unidentified chains shown in Table III could originate from the isotope ^{203}Fr and in the following some support for this statement is provided. The praseodymium target used is from a monoisotopic element and the bombarding energies used were close to Coulomb-barrier energies, which means that the yields are limited into a few fusion evaporation channels. The radon-polonium α decay chains are reasonably well known and for the radium-radon α decay chains the yields are too high. In all of the decay chains the measured half-life of the daughter decay is about the same. And finally the available amount of statistics (688 events obtained for the ground-state-to-ground-state decay) together with the power of the correlation method enables us to look for weak fine-structure decays in the α decay process.

In Fig. 7 experimental excitation energies for the low-lying states in odd-mass bismuth, astatine, and francium isotopes in the region of interest are shown. A general trend is that these states are coming down in excitation energy with decreasing neutron number. Actually some of these states are becoming the ground state, replacing the status of the $(\pi h_{9/2})9/2^-$ state known to be the ground state for most of the odd-even nuclei in this region. A good example of such a situation is ^{195}At in which the proton intruder $(\pi s_{1/2}^{-1})1/2^+$ state becomes the ground state and the $(\pi f_{7/2})7/2^-$ state lies only 32 keV above this ground state [4]. In the daughter nucleus ^{191}Bi the $(\pi f_{7/2})7/2^-$ state lies between the $(\pi h_{9/2})9/2^-$ ground state and the $(\pi s_{1/2}^{-1})1/2^+$ isomeric intruder state. An $E3$ transition was identified to occur between the $(\pi s_{1/2}^{-1})1/2^+$ intruder state and the $(\pi f_{7/2})7/2^-$ state in ^{191}Bi competing with the α decay known to occur between the states of equal spin and parity [4].

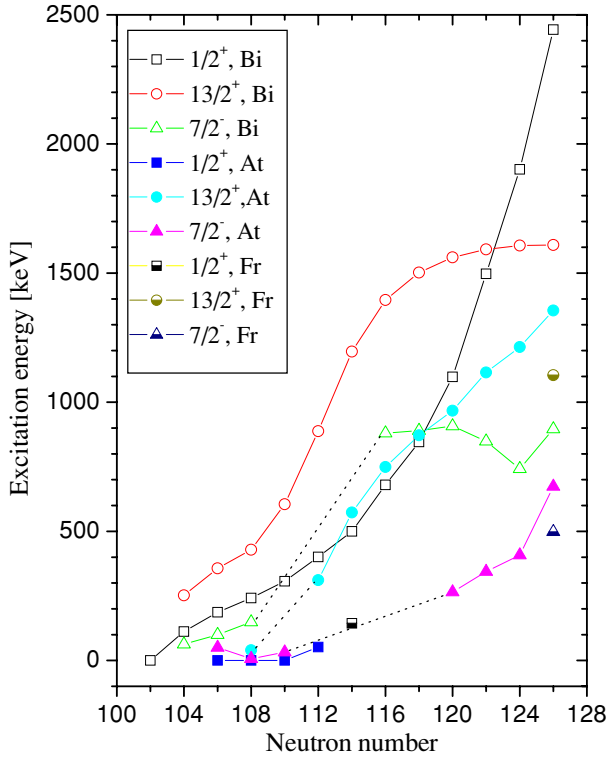

FIG. 7. (Color online) Experimental excitation energies for the low-lying states in odd-mass bismuth, astatine, and francium isotopes in the region of interest. The $9/2^-$ states, in most of the cases the ground states, are not shown.

A possible competition between an α decay and an $E3$ transition could also explain the decay properties of neutron-deficient francium isotopes. An α decay with $E_\alpha = 7227(8)$ keV was measured to proceed with a half-life of 60 ms (see Table III). If a 100% α decay branch is assumed a surprisingly high reduced width value of 208 keV is obtained. The reduced width would be smaller if the state were a $(\pi s_{1/2}^{-1})1/2^+$ intruder state having an $E3$ branch to a possible $(\pi f_{7/2})7/2^-$ state. Both of these states are predicted to come down in energy in Fr isotopes with decreasing neutron number. The $(\pi f_{7/2})7/2^-$ state will decay by a fast $M1$ transition to the $(\pi h_{9/2})9/2^-$ ground state in ^{203}Fr. The $E3$ transition is the only

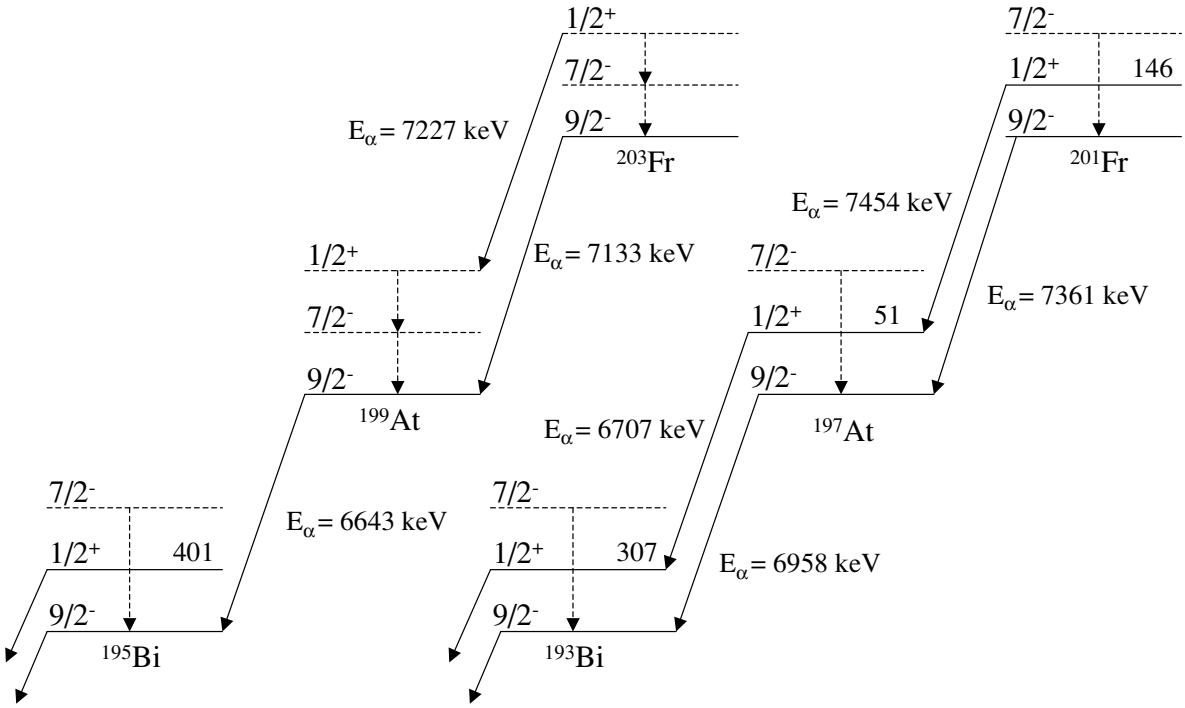

FIG. 8. Suggested α decay schemes belonging to odd-mass francium isotopes are shown.

transition mode that could compete with similar strength with an α decay in this time scale. Another way to have a competing $E3$ transition in this region is a transition between the $13/2^+$ and $7/2^-$ states but this can be ruled out in this case. The decay with $E_\alpha = 7227(8)$ keV was followed by a decay with $E_\alpha = 6643(6)$ keV and $T_{1/2} = 4.3$ s, which are compatible with the decay properties of the $(\pi h_{9/2})9/2^-$ ground state of ^{199}At. The possible unhindered α decay with $E_\alpha = 7227(8)$ keV is feeding the corresponding $(\pi s_{1/2}^{-1})1/2^+$ proton intruder state in ^{199}At but due to the lower α decay energy the α decay from this intruder state cannot visibly compete with the possible $E3$ transition [to the low-lying $(\pi f_{7/2})7/2^-$ state] in the daughter. This $E3$ transition will be followed by a fast $M1$ transition to the $(\pi h_{9/2})9/2^-$ ground state in ^{199}At. From the systematics it can be predicted that the $(\pi f_{7/2})7/2^-$ state should lie well below the $(\pi s_{1/2})1/2^+$ proton intruder state in ^{199}At. The above interpretations are illustrated in Fig. 8.

The α decay with $E_\alpha = 7128(6)$ keV was followed by a decay with $E_\alpha = 6021(6)$ keV. The measured decay properties for the parent activity point to the decay from the ^{203}Fr ground state. On the basis of the measured half-life, the daugher decay can be assumed to originate from the ^{199}At ground state with a reduced width value of 71 keV, implying that the decay is not hindered. Therefore the α decay with $E_\alpha = 6021(6)$ keV could represent a branch to an excited $[\pi h_{9/2} \otimes 2^+]I^-$ state in the daughter nucleus ^{195}Bi. Actually in a recent work an excited state $[\pi h_{9/2} \otimes 2^+]I^-$ at an energy of 620 keV was found [25] for ^{193}Bi, which is close to the value of 635 keV, which can be obtained if the α decay with $E_\alpha = 6021(6)$ keV is occurring as described above.

The α decay with $E_\alpha = 7118(6)$ keV was followed by a decay with $E_\alpha = 6517(6)$ keV. The measured half-life for the parent decay is about twice that measured for the ground-state decay of ^{203}Fr. The measured decay energy for the daughter decay could be due to the fine structure in the ground-state decay of ^{199}At; however, no low-lying excited states (less than 300 keV) in ^{195}Bi have been identified or are expected. For example, the $(\pi f_{7/2})7/2^-$ state cannot lie below the $(\pi s_{1/2}^{-1})1/2^+$ state in ^{195}Bi because a half-life of 87 s has been measured for this α decaying proton intruder state. Therefore at this point it is not possible to associate this decay chain with states in Fr or Bi nuclei.

The α decay of ^{201}Fr was measured with about 10 times lower statistics. Therefore such possible fine structrures suggested to be seen in the α decay of ^{203}Fr and its daughter ^{199}At were not visible in ^{201}Fr.

In conclusion, two new α decaying radium isotopes, ^{201}Ra and ^{202}Ra, were identified and the α decay of ^{203}Ra was studied with improved accuracy. The α decay properties measured for the francium isotopes ^{201}Fr, ^{202}Fr, ^{203}Fr, and ^{204}Fr were confirmed and in many cases with improved precision. For the first time, a $(\pi s_{1/2}^{-1})1/2^+$ proton intruder state was identified in a francium isotope, namely in ^{201}Fr. Tentative evidence for fine structure in the α decay of ^{199}At is presented as well as for α decay from a $(\pi s_{1/2}^{-1})1/2^+$ proton intruder state in ^{203}Fr. It is striking to note how the measured α decay properties of the francium isotopes obtained in the present work point to the same characteristics of the decaying states as their corresponding daughter activities astatines have. Present work and the work [4] suggests the existence of a low-lying $1/2^+$

proton intruder isomeric (ground) state in ^{199}Fr. Because the $9/2^-$ state is associated with the spherical shape and the $1/2^+$ proton intruder state is associated with an oblate character an onset of substantial deformation is expected to occur at neutron number $N = 112$ in odd-mass Fr isotopes.

ACKNOWLEDGMENTS

This work was supported by the Academy of Finland under the Finnish Centre of Excellence Programme 2000–2005 (Project No. 44875, Nuclear and Condensed Matter Physics Programme at JYFL).

[1] A. N. Andreyev *et al*., Phys. Rev. Lett. **82**, 1819 (1999).
[2] A. N. Andreyev *et al*., Nature (London) **405**, 430 (2000).
[3] E. Coenen, K. Deneffe, M. Huyse, P. Van Duppen, and J. L. Wood, Phys. Rev. Letters **54**, 1783 (1985).
[4] H. Kettunen *et al*., Eur. Phys. J. A **16**, 457 (2003).
[5] H. Kettunen *et al*., Eur. Phys. J. A **17**, 537 (2003).
[6] C. N. Davids *et al*., Phys. Rev. Lett. **76**, 592 (1996).
[7] G. L. Poli *et al*., Phys. Rev. C. **63**, 044304 (2001).
[8] H. Kettunen *et al*., Phys. Rev. C **63**, 044315 (2001).
[9] M. Huyse, P. Decrock, P. Dendooven, G. Reusen, P. Van Duppen, and J. Wauters, Phys. Rev. C **46**, 1209 (1992).
[10] J. F. Ziegler, J. P. Biersack, and U. Littmark, *The Stopping and Range of Ions in Solids* (Pergamon Press, New York, 1985).
[11] M. Leino *et al*., Nucl. Instrum. Methods Phys. Res. B **99**, 653 (1995).
[12] A. Rytz, At. Data Nucl. Data Tables **47**, 205 (1991).
[13] J. Wauters, P. Dendooven, M. Huyse, G. Reusen, P. Van Duppen, P. Lievens, and the ISOLDE Collaboration, Phys. Rev. C **47**, 1447 (1993).
[14] T. Enqvist, P. Armbruster, K. Eskola, M. Leino, V. Ninov, W. H. Trzaska, and J. Uusitalo, Z. Phys. A **354**, 9 (1996).
[15] N. Bijnens *et al*., Phys. Rev. Lett. **75**, 4571 (1995).
[16] T. Enqvist, K. Eskola, A. Jokinen, M. Leino, W. H. Trzaska, J. Uusitalo, V. Ninov, and P. Armbruster, Z. Phys. A **354**, 1 (1996).
[17] M. B. Smith *et al*., Eur. Phys. J. A **5**, 43 (1999).
[18] J. O. Rasmussen, Phys. Rev. **113**, 1593 (1959).
[19] G. Audi, O. Bersillon, J. Blachot, and A. H. Wapstra, Nucl. Phys. **A729**, 3 (2003).
[20] P. Möller, J. R. Nix, and K.-L. Kratz, At. Data Nucl. Data Tables **66**, 135 (1997).
[21] Nucl. Data Sheets, **15** (2), 6 (1975).
[22] M. Leino *et al*., Z. Phys. A **355**, 157 (1996).
[23] http://www.nndc.bnl.gov/nudat/.
[24] M. Lach *et al*., Eur. Phys. J. A **9**, 307 (2000).
[25] P. Nieminen *et al*., Phys. Rev. C **69**, 064326 (2004).
[26] H. De Witte *et al*., Eur. Phys. J. A (to be published).